Monthly Notices
of the
ROYAL ASTRONOMICAL SOCIETY

Mon. Not. R. Astron. Soc. **415,** 701–708 (2011) doi:10.1111/j.1365-2966.2011.18747.x

# A new astrometric reduction of photographic plates using the DAMIAN digitizer: improving the dynamics of the Jovian system

V. Robert,[1,2,3★] J.-P. De Cuyper,[4] J.-E. Arlot,[1] G. de Decker,[4] J. Guibert,[5†] V. Lainey,[1] D. Pascu,[6‡] L. Winter[4] and N. Zacharias[6]

[1]*Institut de Mécanique Céleste et de Calcul des Éphémerides IMCCE- Observatoire de Paris, UMR 8028 du CNRS, 77 avenue Denfert-Rochereau, 75014 Paris, France*
[2]*Laboratoire d'Astrométrie Appliquée LASA, 31 rue d'Yerres, 91230 Montgeron, France*
[3]*Institut Polytechnique des Sciences Avancées IPSA, 7-9 rue Maurice Grandcoing, 94200 Ivry-sur-Seine, France*
[4]*Royal Observatory of Belgium ROB, avenue Circulaire 3, B-1180 Uccle, Belgique*
[5]*Laboratoire Galaxie - Etoile - Physique - Instrumentation - Observatoire de Paris, UMR 8111 du CNRS, 61 avenue de l'Observatoire, 75014 Paris, France*
[6]*United States Naval Observatory USNO, 3458 Massachusetts Ave NW, Washington, DC 20392, USA*

Accepted 2011 March 17. Received 2011 March 13; in original form 2011 January 8

**ABSTRACT**

The astrometric monitoring of the natural planetary satellites is an important step to assess the formation and the evolution of these systems. However, in order to quantify relevant gravitational effects such as tidal forces, it is necessary to have very accurate observations over a long time interval. Unfortunately, the accuracy is decreasing as one considers older observations. To solve this issue, digitizing of old photographic plates is an attractive method, but a high accuracy in the measurement and the reduction of those plates is absolutely necessary.

We have developed methods and algorithms adapted to specific plates provided by USNO, using the DAMIAN digitizer of ROB. From a set of 35 plates taken in 1974, we have been able to produce measurements with an accuracy better than 0.08 μm and after reduction using the UCAC2 catalogue, rms residuals of 35 mas (1.7 μm) for intersatellite positions (when the original reduction provided 100 mas) and of 65 mas for equatorial RA and Dec. positions (which were not possible to get with the original reduction). First results on the dynamics of the satellites and of the planet Jupiter are provided.

**Key words:** techniques: image processing – astrometry – ephemerides – planets and satellites: general.

## 1 INTRODUCTION

The study of the dynamics of the natural planetary satellite systems needs astrometric observations, sampled over an interval of time as long as possible, in order to quantify the long period terms which may help to analyse the evolution of the motion. The search of old data may be useful for this purpose. However, the accuracy of old observations is mostly poor and does not provide any information on small effects in the motion of the satellites.

A new reduction of good photographic plates may be a solution and a project has been initiated for that purpose between the Institut de Mécanique Céleste et de Calcul des Éphemerides (IMCCE, Paris Observatory, France), the Royal Observatory of Belgium (ROB) and the US Naval Observatory (USNO, Washington DC, USA). The ROB had the aim to preserve the historic and scientific information contained in aerial and astro photographic archives, both on film or glass plates and then to provide scientists the content of these photographic images in a digital form for further analysis (De Cuyper, Winter & Vanommeslaeghe 2004; De Cuyper & Winter 2005, 2006; De Cuyper et al. 2009). For that purpose, the DAMIAN machine (Digital Access to Metric Images Archives Network) was acquired by the Royal Observatory of Belgium. In autumn 2007 the digitizer was installed and housed in a temperature- and humidity-stabilized clean room with adjacent archive room. The DAMIAN machine can digitize photographic images up to 350-mm wide on glass plates, film sheets and film rolls. The mechanical subsystem includes an automatic plate holder assembly, a plate tray exchange robot with plate tray magazine and turntable for photographic glass plates and film sheets and an automatic film roll transport system. These custom made devices allow a rapid change and loading into focus of the photographs to be digitized without manual intervention.

In order to evaluate the scientific ability of the machine for astrometric purposes, an international collaboration has been set up

★E-mail: robert@imcce.fr
†GEPI retired.
‡USNO retired.

between the three partners: ROB, USNO and the Paris Observatory (IMCCE/LASA). The ROB provides the digitizations and its considerable expertise with the digitizer systems, calibration of camera and measure system for the most precise digitization. The USNO provides astrophotographic plates of high quality for the science programme (Pascu 1977, 1979, 1994) and its astrometric expertise with star catalogues and reduction methods. The IMCCE/LASA analyses the data and provides its expertize in image analysis, reduction methods and its knowledge of astrometry, ephemerides and dynamics of natural satellites. This paper presents the work which has been done to solve many problems before getting the needed accuracy from the machine, and the results obtained with the set of 35 plates of the Galilean satellites made in 1974.

## 2 DAMIAN FEATURES

### 2.1 Hardware

Fig. 1 shows the DAMIAN digitizer as on 2009 March. The machine consists of a granite based Aerotech ABL 3600 open frame air-bearing *XY* positioning table, with an automatic plate holder assembly suited for mounting glass plates and film sheets up to 350-mm wide. The granite base measures 1.5 m × 1.2 m × 0.2 m. Extended with an automatic film roll transport system and an automatic plate tray handling and storage assembly with plate rotator, the DAMIAN digitizer is able to process automatically almost all known transparent photographic material.

The optical unit consists of a BCi4, 12 bit CMOS Camera from C-Cam Vector International, mounted on a Schneider Xenoplan telecentric 1:1 objective. This system is attached to the *Z*-axis above the *XY* table. The 2D CMOS Camera provides images with 1280 × 1024 pixels of 7 μm × 7 μm. The photographic images are illuminated from below with very bright Light Emitting Diode's (LED lifetime min. 50 000 h), controlled by a high precision DC power supply.

The position of the *XY* table is read by Heidenhain encoders. The linearity and orthogonality of the (*X*, *Y*) axes were calibrated by Aerotech using a laser interferometer. The local *XY* table positioning repeatability (how closely the table can return to an initial position following movement over the entire *X*–*Y*) was measured with a capacitance by the manufacturer at 0.008 μm. The fitted object positions in different digitizations (7 μm × 7 μm pixels) of the same test plate were found to repeat within 0.07 μm. These results

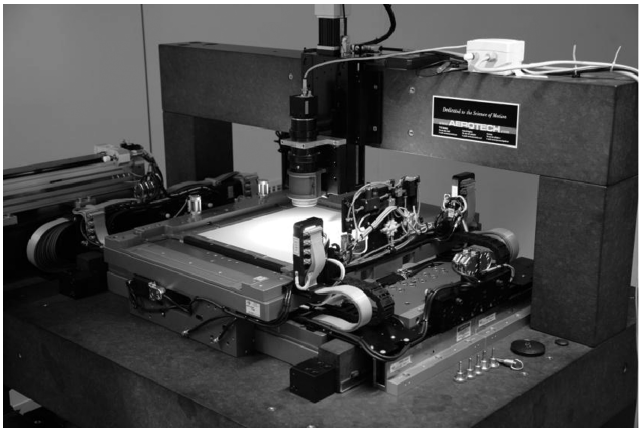

**Figure 1.** The DAMIAN digitizer at ROB, Brussels.

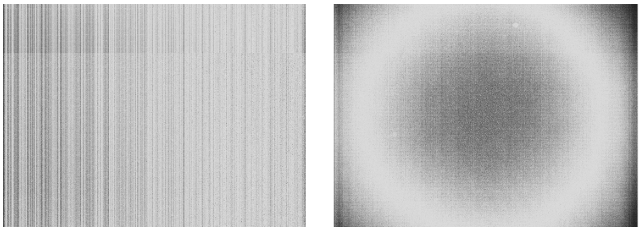

**Figure 2.** DAMIAN mean dark (left) and mean flat (right).

are even better than previously obtained from the StarScan machine at USNO (Zacharias et al. 2008).

In order to reach and maintain a high geometric and radiometric accuracy, the digitizer is placed in an air-conditioned clean room, at a temperature of 20°C ± 0.05°C and a relative humidity of 50 per cent RH ± 1 per cent RH.

### 2.2 Digitizing process

Most of the DAMIAN functions are computer controlled. At the beginning of each plate digitization, the photographic plate is put automatically into focus by pressing it up against the counterpressure plate. The illumination is set to just below saturation on the plate's sky background by adjusting the DC power supply unit to the LED. The plate is digitized automatically in step and stare mode with steps corresponding to exactly 704 pixels in the *X* and *Y* directions in a zigzag pattern. After the plate is completely digitized, the plate holder is unclamped and the plate automatically removed. The time needed to digitize a single plate of 12 cm × 17 cm is 9 min. Fig. 2 shows mean dark and mean flat images, obtained by averaging a 1000 individual images taken at the same integration time of 15 ms, that are used to correct the individual raw plate images. An overall mosaic FITS image of the whole photographic plate is also generated from the inner non overlapping (704 × 704 pixels) part of the individual images. The stepping of 704 pixels was chosen in order to restrain the optical distortion effects in the non-overlapping parts of the sub-images.

### 2.3 Geometric correction of the camera optical distortion

In order to correct for the optical distortion of the objective/detector unit, seven-parameter third order polynomials (equation 1, Winter 2008) are used to calculate corrected *x* and *y* plate coordinates as a function of the measured plate coordinates $x_0$ and $y_0$ with respect to the centre of the individual subimage:

$$\begin{aligned} x &= \rho_x x_0 + \nu_x y_0 - \mathrm{d}\Delta_x \left(3x_0^2 + y_0^2\right) - \mathrm{d}\Delta_y (2x_0 y_0) \\ &\quad + \mathrm{d}x_0 \left(x_0^2 + y_0^2\right), \\ y &= \rho_y y_0 + \nu_y x_0 - \mathrm{d}\Delta_x (2x_0 y_0) - \mathrm{d}\Delta_y \left(x_0^2 + 3y_0^2\right) \\ &\quad + \mathrm{d}y_0 \left(x_0^2 + y_0^2\right), \end{aligned} \tag{1}$$

where $\rho_x$ and $\rho_y$ are scales on the *XY* plate axes; $\nu_x$ and $\nu_y$ are rotation terms mixed with non-orthogonality and corresponding plate scales; $d\Delta_x$ and $d\Delta_y$ are distortion offsets; *d* is the third order distortion term. In the same temperature and humidity conditions, these parameters were found to be stable to within $1\sigma$ of their individual formal errors.

As the positioning repeatability of the *XY* table is two orders of magnitude better than the resolution of the digital camera, these optical distortion parameters are evaluated by stepping a well exposed

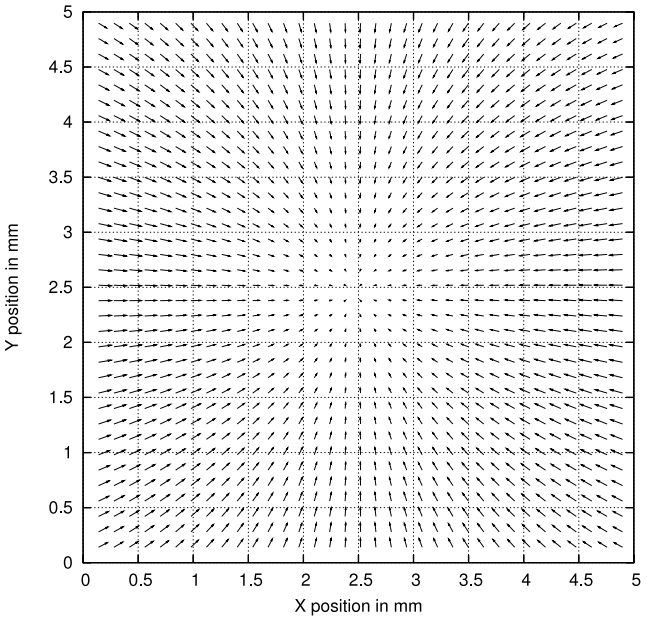


**Figure 3.** The correction of the optical distortion of the objective/camera unit, in the inner 704 × 704 pixels field of view of the camera, shown as vectors enlarged 100 times (the largest vector is about 1.5-μm long).

star in the field of view of the digital camera. Using the StarScan-View software (Winter 2005) the aimed star position is fitted and a table is generated containing the fitted $(x_i, y_i)$ star position as function of the corresponding $(X_i, Y_i)$ table position. A least-squares fitting procedure is used to calculate the seven parameters of equation (1). Fig. 3 shows the corrections of the optical distortion of the objective/camera unit in the central 704 × 704 pixels (corresponding to 5 × 5 mm) field of view of the camera as vectors scaled by a factor of 100, thus the largest vector is about 1.5-μm long. The magnitude of the optical correction, at the edges of a 704 × 704 pixels sub-image, is 1.26 μm on the $X$-axis and 0.78 μm on the $Y$-axis. The difference between the two is due to the non-zero other terms in equation (1) causing a slight anisotropy between the $x$ and $y$ coordinates.

## 3 ASTROMETRIC TEST PROGRAMME

### 3.1 The digitized plates

One of the current DAMIAN digitizer programmes deals with the digitizing and the analysis of photographic plates of planetary satellites. Our intention is to digitize a subset of the USNO plates archive; 35 plates from 1974, consisting of 100 exposures with a limiting V magnitude of 10 to 12. These exposures were taken with the USNO 26-inch refractor on Kodak 103aG glass plates by Pascu (1977, 1979, 1994). A Schott GG14 filter was used in combination with a neutral density filter to reduce the brightness of the planet and Galileans to that of ninth V magnitude stars. This subset was chosen because these plates were already previously measured twice; manually, using a MANN two-screw measuring machine (Arlot 1982) and the trail-scale reduction method (Pascu 1977) and, automatically using a PDS digitizer (Arlot 1980). Additionally because the ephemerides of the Galilean satellites are known accurately and studied extensively at IMCCE, a new reduction of these plates, leading to right ascension (RA) and declination (Dec.) of the satellites, and using new star catalogues permit us to improve the astrometric precision, to improve the satellite orbital motions, and to infer the accuracy of Jupiter's ephemeris. Moreover, this new reduction is a useful test of the digitizer which will tells us if the remaining part of the USNO plate archive should be digitized and analysed.

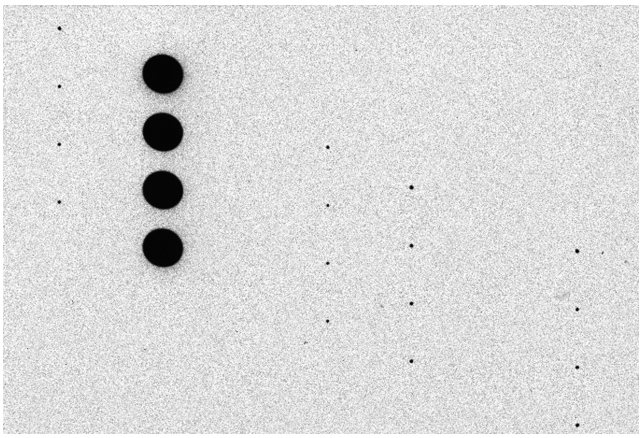

**Figure 4.** Centre of the USNO Galilean plate n°0318.

### 3.2 Data extraction

Each USNO plate contains three to seven exposures shifted in the Dec. direction. Fig. 4 shows the centre of the USNO Galilean plate n°0318 digitized with the DAMIAN machine.

In order to obtain a quick result, the $(x, y)$ of the Galilean satellites and the stars were extracted from the mosaic FITS images by means of a specific process. First the Source Extractor software (Bertin & Arnouts 1996) was used to create a list of objects detected on the plates; thousands of possible sources were generally detected on each plate, even after a selection for circular objects and a magnitude constraint. Hence, the objects assumed to be present in the field needed to be identified from existing catalogues in order to select only the real physical objects on the plates. The plate positions obtained were corrected for the optical distortion introduced by the objective/camera unit during the digitization and transformed to celestial coordinates using a plate scale of 20.84 arcsec mm$^{-1}$, after taking into account various corrections such as the aberration of light (Kaplan et al. 1989) and the atmospheric refraction.

Equatorial (RA, Dec.) and intersatellite astrometric positions were determined in an ICRF geocentric reference frame in order to be easily compared with current ephemerides. According to the high quality of the USNO plates, and to the accurate planetary and Galilean ephemerides used, the (RA, Dec.) (O−C) differences between observed and computed (theoretical) positions were expected to be better than 50 mas (Fienga 1998). Note that 1 mas $\simeq$ 3 km at the Jupiter Galilean system. This accuracy was already achieved but only with intersatellite results (systematic effects due to the planet position are eliminated with this kind of reduction).

### 3.3 Repeatability of the DAMIAN digitizer positioning

In order to obtain an estimate of the positioning repeatability of the DAMIAN digitizer, the USNO Galilean plate n°2114, containing five exposures of 20 s each, was digitized several times in direct and reverse modes (D–R) with the DAMIAN machine. The reverse mode is scanning a plate at 180° to the usual (direct) orientation. This is an important method for detecting and eliminating machine-caused systematic effects, and in particular those that depend on

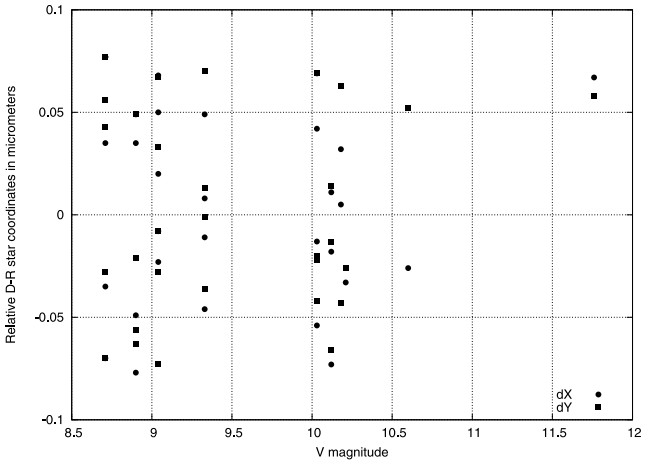


**Figure 5.** Examples of positioning repeatability measures for two D–R DAMIAN digitizations.

magnitude. Thus we chose to perform a plate-to-plate analysis from successive scans; in fact, the objects on this plate do not need to be identified but they are fixed and supposed to be measured at the same relative positions. The test compares the d$X$ and d$Y$ differences between the same relative positions calculated from the successive direct and reverse digitizations. We used six UCAC2 (Zacharias et al. 2004) and BSS (Urban, Zacharias & Wycoff 2004) stars on each exposure to perform the test.

Fig. 5 shows examples of d$X$ and d$Y$ results of positioning repeatability measures for UCAC2 stars with respect to star BSS_50047604, as a function of magnitude for two DAMIAN digitizations in direct and reverse modes. These results are representative of the D–R digitizations we analysed. We calculated a simple matrix transformation on the coordinates from the reverse scan so that the two sets of coordinates could be compared. This method let us know whether machine-based terms (magnitude effect during scan process) should be considered.

Application to position of stars shows that there are no obvious machine-based terms with the two D–R DAMIAN digitizations, at our level of measurement accuracy. We estimate positioning repeatability better than 0.08 μm. Actually these errors come mostly from fitting uncertainties associated to the USNO plate. We estimate the fitting precision to a few hundredths of micrometers, indicating that the current analysis is limited because the fitting errors dominate.

### 3.4 Stability of the data extracted from successive observations

In order to evaluate the stability of the data extraction, several plates taken successively during the same night were digitized with the DAMIAN machine and compared with the results obtained from previous measurements. As the PDS microdensitometer raw data were not available, we only compared the MANN manual measurements with the data extracted from the DAMIAN digitizations. For the derived intersatellite distances JI − JII, JI − JIII and JI − JIV, (O−C) values and plate average dispersions $\sigma_s$ were calculated by using the theoretical intersatellite separations given by the L2 Galilean ephemeris (Lainey et al. 2009). Table 1 shows the $\sigma_s$ dispersions for the USNO Galilean plates n°0306 and n°0307, n°0326 and n°0327, n°0336 and n°0337, resulting in eight observations for each dispersion measurement. Each plate pair was obtained on one night respectively in 1974 September, October and November. Due to the limited number of data, note that the $\sigma_s$ dispersion is not fully significant. Nevertheless it still provides an interesting indicator of satellite measurement errors.

**Table 1.** Intersatellite plate average separation dispersions obtained from USNO Galilean plates with the (a) MANN manual and (b) DAMIAN methods.

| Plate pairs | | $\sigma_s$ separation dispersion in mas | | | | | |
|---|---|---|---|---|---|---|---|
| Plate | | 0306 | 0307 | 0326 | 0327 | 0336 | 0337 |
| JI–JII | (a) | 55 | 91 | 96 | 67 | 40 | 69 |
| | (b) | 30 | 30 | 66 | 62 | 20 | 32 |
| JI–JIII | (a) | 49 | 43 | 91 | 102 | 65 | – |
| | (b) | 22 | 13 | 59 | 57 | 48 | – |
| JI–JIV | (a) | 58 | 64 | 118 | 102 | 64 | 54 |
| | (b) | 11 | 14 | 66 | 64 | 49 | 51 |

We suppose here that the ephemeris errors remain constant during the small interval of time that was needed to take these successive plate exposures. Hence, the differences between the $\sigma_s$ dispersions within the same plate pair should be minimum. Also, if the orbits had no error, the differences would be mainly due to measuring errors and atmospheric seeing variations from exposure to exposure. The results presented in Table 1 allow us to appreciate the quality of the forthcoming astrometric results. We remark that the residuals of the MANN manual measurements are larger and even not stable within one night, indicating that they are less reliable. The DAMIAN digitizations produce more stable and coherent results.

### 3.5 Astrometric reductions

#### *3.5.1 Catalogue reduction*

We calibrated the field of the USNO observations by tying the measured ($x$, $y$) star plate coordinates to a reference star catalogue. We use a traditional method of plate constants that we call 'star link method'.

The conventional plate model consists of a full second or third order polynomial expansion to compensate for various instrumental and physical effects. Because this model needs a large number of reference stars to fit the plate parameters and because this model does not allow us to separate the contributions of the various effects, here we used a functional plate model with a minimal number of plate parameters after correcting the ($x$, $y$) measurements for all known instrumental and spherical effects, including the total atmospheric refraction and the parallax and aberration effects. It is justified with the USNO plates because of the small number of reference stars available, usually less than seven stars. We used the following first order reduction equations modelling scales $\rho_x$ and $\rho_y$, orientations $\theta_x$ and $\theta_y$, offsets $\Delta_x$ and $\Delta_y$ to calculate tangential ($X$, $Y$) coordinates for each reference star measured on the plate:

$$X = \rho_x \cos\theta_x x - \rho_y \sin\theta_x y + \Delta_x,$$
$$Y = \rho_x \sin\theta_y x + \rho_y \cos\theta_y y + \Delta_y. \quad (2)$$

Theoretical star positions obtained from reference catalogues were converted to tangential coordinates using the gnomonic projection. Differences between measured and theoretical tangential positions were minimized using weighted least-squares solutions.

In order to perform the instrumental calibration, we evaluated with Praesepe and Pleiades cluster images (50 reference stars available for each exposure) different effects such as the telescope instrumental distortion, the plate tilts and the coma-magnitude effects.

We incorporated in these equations a third order distortion term, two plate tilt terms and two coma-magnitude $C_x x(m - m_0)$ and $C_y y$ $(m - m_0)$ terms where $m$ is the star magnitude and $m_0$ the mean magnitude available on the plate, to estimate each effect contribution. We found distortion and tilt terms to be insignificant. We also found two constant coma-magnitude terms $C_x = -0.67 \pm 0.06\,\mu\mathrm{m}^{-1}\,\mathrm{mag}^{-1}$ and $C_y = -0.92 \pm 0.06\,\mu\mathrm{m}^{-1}\,\mathrm{mag}^{-1}$ with diaphragmed (16-inch aperture) observations and $C_x = -1.55 \pm 0.03\,\mu\mathrm{m}^{-1}\,\mathrm{mag}^{-1}$ and $C_y = -0.67 \pm 0.06\,\mu\mathrm{m}^{-1}\,\mathrm{mag}^{-1}$ with full aperture (26 inch) observations.

Once we take into account the mentioned instrumental and spherical corrections before adjustment, we use equation (2) with determined constants to calculate tangential $(X, Y)$ coordinates for each satellite, then we correct for the phase effect (Lindegren 1977) and we obtain the equatorial (RA, Dec.) astrometric positions by using the gnomonic inverse projection. (O−C) residuals are calculated for the Galilean positions measured according to a J2000 geocentric frame and using the L2 Galilean ephemerides (Lainey et al. 2009). We will also use equatorial (RA, Dec.) positions to compute intersatellite positions with respect to the centre of the discs.

### 3.5.2 *The $\rho_x$ and $\rho_y$ scale factors*

The scale factors on both $X$ and $Y$ axes are the main indicators that characterize the isotropy of the field and in consequence, the robustness of the reduction model used. In the case of MANN manual and PDS microdensitometer measurements and in order to use the trail-scale method, the scale factors were calculated with diaphragmed Praesepe and undiaphragmed Pleiades plates taken in 1974 and 1994. Each exposure contains about 50 reference stars. The scale factors were assumed to be stable and equal for all the plates taken with the same telescope: $\rho_x = \rho_y = 20.843 \pm 0.002$ arcsec $\mathrm{m}^{-1}$. This is the scale value of the 26-inch diaphragmed to 16-inch aperture, and corrected for differential refraction (Josties et al. 1974). Otherwise, if the measurements are corrected for total refraction, a scale value of $\rho_x = \rho_y = 20.839 \pm 0.002$ arcsec $\mathrm{mm}^{-1}$ should be used.

In the case of the DAMIAN star link method, we determined the scale factors with the same Praesepe and Pleiades images by identifying the corresponding parameters from the least-squares solution of our first order reduction model. We assume that the scale factors on both $X$ and $Y$ axes are not equal but depend on each individual observation, and we assume that if they are equal (not necessarily true), it would indicate an isotropy.

Without the corrections mentioned above, the scale factors in $X$ and $Y$ are quite different because the constants tend to correct the effective anisotropy of the field. Fig. 6 shows the anisotropy through the scale factors on both $X$ and $Y$ axes. The error bars are $1\sigma$, representative of the single-exposure measurement and of the plate and catalogue errors. The errors are comparable to the size of the data points.

Once we take into account the instrumental and spherical corrections, and in particular the total atmospheric refraction, the coma-magnitude effects and the aberration of light, the scale factors become equivalent for each individual Praesepe observation. Fig. 7 shows the isotropy through the scale factors once the corrections are applied. The error bars are $1\sigma$, representative of the single-exposure measurement and of the plate and catalogue errors. The errors are comparable to the size of the data points.

We estimate the following mean values: $\bar{\rho_x} = \bar{\rho_y} = 20.8388 \pm 0.0003$ arcsec $\mathrm{mm}^{-1}$. This is the scale value of the 26-inch diaphragmed to 16-inch aperture, and outside the atmosphere. To apply this scale factor, the measurements must be corrected for total atmospheric refraction. This mean value is lower than the previous 20.843 arcsec $\mathrm{mm}^{-1}$ scale factor determined to use the trail-scale method inside the atmosphere because in this last case, the atmosphere acts as an optical element in increasing the scale value. Nevertheless the mean 20.8388 arcsec $\mathrm{mm}^{-1}$ scale factor is very close to the previous 20.839 arcsec $\mathrm{mm}^{-1}$ value. In the following order of magnitude, the total atmospheric refraction brings the $\rho_y$ value to the $\rho_x$ value but a slight difference remains. The coma-magnitude correction finally tightens the scale values, and the aberration of light shifts the $\rho_x$ and $\rho_y$ scale factors.

We reproduced the same analysis with the undiaphragmed Pleiades images and we estimate the following mean values: $\bar{\rho_x} = \bar{\rho_y} = 20.8514 \pm 0.0003$ arcsec $\mathrm{mm}^{-1}$. This is the scale value of the undiaphragmed 26 inch and inside the atmosphere. To apply this scale factor, the measurements must be corrected for differential atmospheric refraction.

We demonstrate here that it is possible to reduce plates with very few reference stars by making theoretical corrections and using a unique $\rho$ factor for the isotropic scale. We also verified that the $\theta_x$ and $\theta_y$ orientation terms were equivalent for each individual observation; in consequence, we have two parameters less in

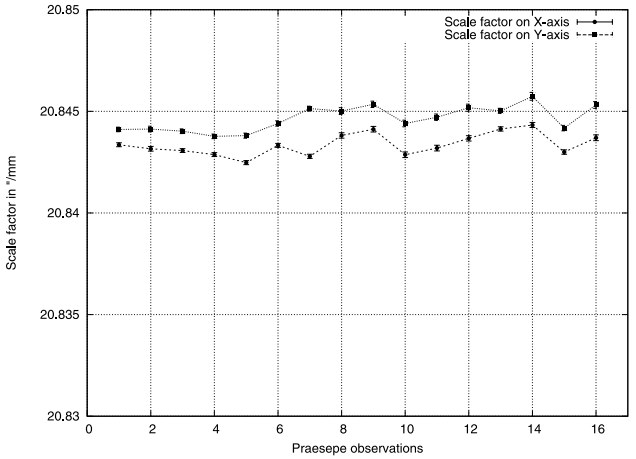


**Figure 6.** Scale factors in $X$ and $Y$ obtained with Praesepe observations and without corrections.

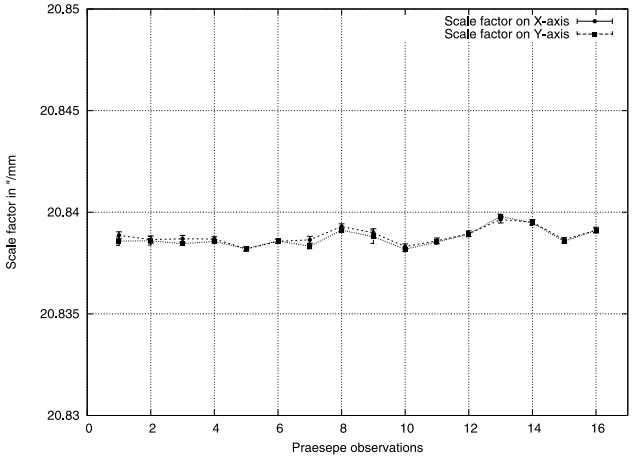


**Figure 7.** Scale factors in $X$ and $Y$ obtained with Praesepe observations and with corrections applied.

equation (2) and the plate model reduces to only four parameters (modelling mean scale $\rho$, mean orientation $\theta$, offsets $\Delta_x$ and $\Delta_y$), strengthening the solution:

$$X = \rho \cos\theta x - \rho \sin\theta y + \Delta_{x,}$$
$$Y = \rho \sin\theta x + \rho \cos\theta y + \Delta_{y.} \quad (3)$$

## 4 ASTROMETRIC RESULTS IN (RA, DEC.) POSITIONS

One key point in the DAMIAN measurements associated with the star link reduction method is to provide the positions of the satellites as RA and Dec. in J2000 ICRF reference frame. Of course, intersatellite measurements are sufficient for the study of the dynamics of the satellites and may be deduced from these (RA, Dec.) values. However, the (RA, Dec.) positions of the satellites permit the determination of (RA, Dec.) positions of Jupiter indirectly from the satellites; this is required because direct measurements of the planet from the photographic plates involve large systematic errors.

We present here the results obtained from 35 plates (100 individual exposures) made during the opposition of Jupiter in 1974. We were not able to compare with manual measurements since the trail scale reduction method, with no link to reference stars, was not able to provide (RA, Dec.) positions. Comparisons are only possible for intersatellite positions and given in Fig. 8 and Table 2 which show the accuracy of L2 ephemerides through the average individual (O−C) values with respect to the barycentre of the observed satellites, and the stability of the DAMIAN measures through the values of the dispersions. Averages are the square roots of the mean squared sigmas. Note that the dispersion for all the series is smaller than with the MANN measurements (Arlot 1982).

**Table 2.** Details of the intersatellite (O−C) in mas with DAMIAN digitizations: USNO Galilean plates of 1974.

| Satellite | $\overline{(O-C)}_{\alpha\cos\delta}$ L2 | $\sigma_{\alpha\cos\delta}$ | $\overline{(O-C)}_{\delta}$ L2 | $\sigma_{\delta}$ |
|---|---|---|---|---|
| JI | 3 | 30 | 10 | 32 |
| JII | 3 | 32 | −8 | 32 |
| JIII | 7 | 36 | 9 | 32 |
| JIV | −13 | 48 | −11 | 31 |
| Average | 0 | 37 | 0 | 32 |

Let us come now to equatorial (RA, Dec.) positions. In order to calculate the (O−C) values and the dispersion, we need to use an ephemeris of Jupiter. We know that the external error of L2 ephemeris is about 15 mas and one should also keep in mind that the Jupiter ephemeris error will be superposed with the errors from the reduction and the digitization. We used four Jupiter ephemerides: DE421 (Folkner, Williams & Boggs 2008), INPOP06 (Fienga et al. 2008), INPOP08 (Fienga et al. 2009) and INPOP10 (Fienga et al. 2010). Residuals are provided in Fig. 9 and Tables 3, 4, 5 and 6, in mas.

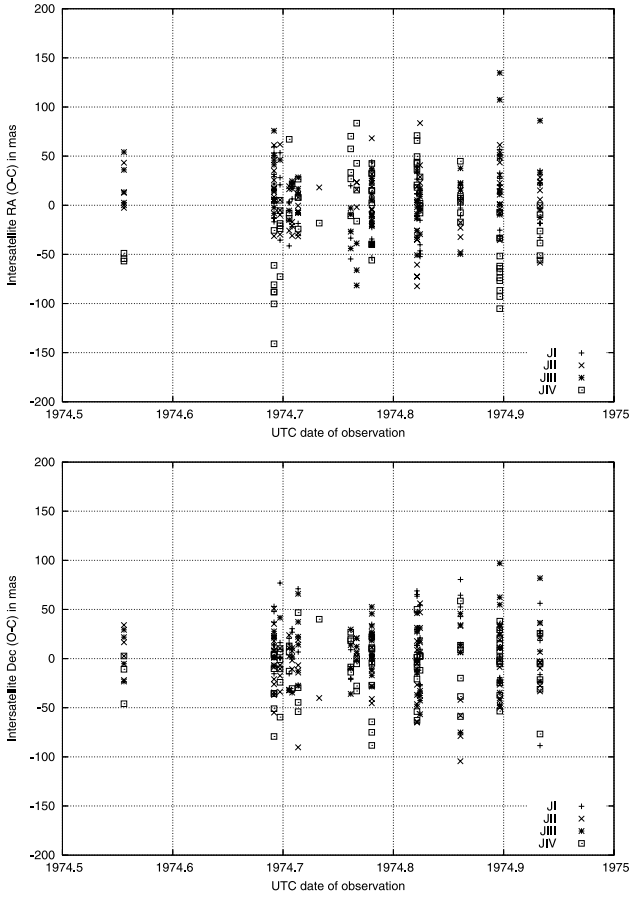


**Figure 8.** Intersatellite (O−C) with DAMIAN digitizations: USNO Galilean plates of 1974.

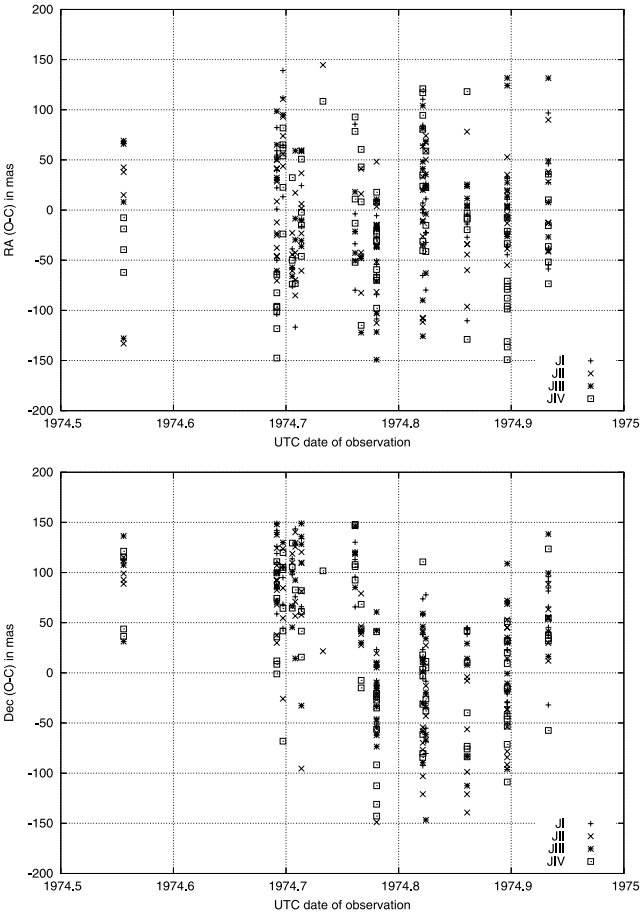


**Figure 9.** (RA, Dec.) (O−C) according to the DE421 theory and with DAMIAN digitizations: USNO Galilean plates of 1974.

**Table 3.** Details of the (RA, Dec.) (O−C) in mas according to the DE421 theory and with DAMIAN digitizations: USNO Galilean plates of 1974.

| Satellite | $\overline{(O-C)}_{\alpha\cos\delta}$ DE421\L2 | $\sigma_{\alpha\cos\delta}$ | $\overline{(O-C)}_{\delta}$ DE421\L2 | $\sigma_{\delta}$ |
|---|---|---|---|---|
| JI | −6 | 54 | 41 | 65 |
| JII | −6 | 55 | 21 | 73 |
| JIII | 0 | 63 | 36 | 70 |
| JIV | −20 | 67 | 17 | 70 |
| Average | −8 | 60 | 29 | 70 |

**Table 4.** Details of the (RA, Dec) (O−C) in mas according to the INPOP06 theory with DAMIAN digitizations: USNO Galilean plates of 1974.

| Satellite | $\overline{(O-C)}_{\alpha\cos\delta}$ INPOP06\L2 | $\sigma_{\alpha\cos\delta}$ | $\overline{(O-C)}_{\delta}$ INPOP06\L2 | $\sigma_{\delta}$ |
|---|---|---|---|---|
| JI | −9 | 54 | 34 | 68 |
| JII | −10 | 56 | 14 | 70 |
| JIII | 1 | 63 | 39 | 72 |
| JIV | −20 | 64 | 10 | 70 |
| Average | −10 | 59 | 24 | 70 |

**Table 5.** Details of the (RA, Dec.) (O−C) in mas according to the INPOP08 theory with DAMIAN digitizations: USNO Galilean plates of 1974.

| Satellite | $\overline{(O-C)}_{\alpha\cos\delta}$ INPOP08\L2 | $\sigma_{\alpha\cos\delta}$ | $\overline{(O-C)}_{\delta}$ INPOP08\L2 | $\sigma_{\delta}$ |
|---|---|---|---|---|
| JI | 65 | 52 | 91 | 67 |
| JII | 64 | 55 | 82 | 77 |
| JIII | 61 | 73 | 91 | 69 |
| JIV | 40 | 76 | 81 | 71 |
| Average | 57 | 64 | 86 | 71 |

**Table 6.** Details of the (RA, Dec.) (O−C) in mas according to the INPOP10 theory with DAMIAN digitizations: USNO Galilean plates of 1974.

| Satellite | $\overline{(O-C)}_{\alpha\cos\delta}$ INPOP10\L2 | $\sigma_{\alpha\cos\delta}$ | $\overline{(O-C)}_{\delta}$ INPOP10\L2 | $\sigma_{\delta}$ |
|---|---|---|---|---|
| JI | 1 | 54 | 31 | 69 |
| JII | −1 | 54 | 11 | 71 |
| JIII | 9 | 65 | 34 | 73 |
| JIV | −15 | 69 | 9 | 71 |
| Average | −2 | 61 | 21 | 71 |

Fig. 9 shows the difference of (RA, Dec.) coordinates of individual satellites and plates, thus observed positions (from DAMIAN digitizations and reduced to UCAC2 reference stars) versus positions calculated from the DE421 ephemeris. Offsets are particularly seen for the Dec. coordinate as a function of epoch. Local systematic errors of the reference star catalogue could explain part of these offsets. The epoch difference between these 1974–75 plates and the central epoch of the reference stars (around 1990 to 1995) is up to about 20 yr. Expected systematic errors of the reference stars at a 1975 epoch are about 15–40 mas. The data shown in Fig. 9 span about 15° along the path of Jupiter, thus each epoch data is linked to a different set of reference stars. With only about 7–15 reference stars per field the astrometric solution can be affected by accidental large errors of individual reference stars. Magnitude and particularly colour dependant systematic errors in the telescope optics are other possible causes of the offsets seen in Fig. 9 and further investigations are planned. Offsets in the centre-of-mass of the Jupiter system (DE421 theory errors) can not be ruled out by the data shown either. It is advisable to use the intersatellite data as shown in Fig. 8 which will be free of these effects because the same set of reference stars is used in the astrometric solution and a zero-point offset in the absolute coordinates is canceled out in coordinate differences data.

The average (O−C) values for the 100 observations made during the 1974 opposition of Jupiter are very small in RA for DE421, INPOP06 and INPOP10, and larger in Dec. (slightly smaller for INPOP10). The external error of DE421 (and INPOP06 and INPOP10) is supposed to be around 10 mas (Folkner et al. 2008) but we may deduce from our results that this external error is realistic in RA but reaches 28 mas in Dec. INPOP08 shows a much larger external error, nevertheless this is in agreement with the difference of 240 km (80 mas) between INPOP06 and INPOP08 provided by Fienga et al. (2009). It is interesting to see that these observations are very useful for the evaluation of the accuracy of the ephemerides of Jupiter since they have not been used for the fit of the numerical integrations leading to DE421, INPOP06, INPOP08 and INPOP10.

In addition, we can see that intersatellite $\sigma_{\delta}$ dispersion values are smaller than intersatellite $\sigma_{\alpha\cos\delta}$. But equatorial $\sigma_{\delta}$ dispersion values are larger than equatorial $\sigma_{\alpha\cos\delta}$. Such a systematic error in the declinations was found by Pascu & Schmidt (1990) when the authors reduced USNO observations of the Saturn system. No cause due to the photographic observations could be found nor to the reduction method.

## 5 CONCLUSION

We have demonstrated the value of a new astrometric analysis of old photographic plates, resulting from their accurate measurement with the DAMIAN digitizer. We analysed a complete series of photographic plates of the Galilean satellites taken at USNO during the apparition of Jupiter in 1974 and extracted all the important information contained in the plate data. We were able to correct for instrumental and spherical effects during the reduction, decreasing the number of unknown parameters by using the same scale factor and orientation in $X$ and $Y$.

The new reduction, using new astrometric catalogues, provided final accurate positions. These astrometric positions of the Galilean satellites were not only more accurate than those previously derived from manual measurements, but provided new information due to the star link reduction; we obtained equatorial RA and Dec. positions of the Galileans, allowing us to deduce positions of Jupiter indirectly through accurate ephemerides of the Galilean satellites. Finally, we compared these astrometric positions of Jupiter to the best current ephemerides of the planet. Depending on the ephemeris, we obtained residuals between a few tens of mas, to better than 100 mas.

The USNO archive contains more plates taken in the interval 1967–98 and the present work has demonstrated that a new analysis of these plates will provide valuable data for the dynamics of the Galilean satellite system and of Jupiter itself. In addition, plates of the Saturnian system are also available and will be analysed soon.

## ACKNOWLEDGMENTS

We thank the Royal Observatory of Belgium and its director Ronald Van der Linden for allowing us to use the DAMIAN digitizer and

the US Naval Observatory for sending their plates for digitization and making plateholders. We thank IMCCE, the scientific council of Paris Observatory and the CNRS for supporting this project.

## REFERENCES

Arlot J. E., 1980, A&A, 86, 55
Arlot J. E., 1982, PhD thesis, Observatoire de Paris
Bertin E., Arnouts S., 1996, A&AS, 117, 393
De Cuyper J. P., Winter L., Vanommeslaeghe J., 2004, in Shopbell P., Brilton M., Ebert R., eds, ASP Conf. Ser. Vol. 314, ADASS XIII, The D4A digitiser. Astron. Soc. Pac., San Francisco, p. 77
De Cuyper J. P., Winter L., 2005, in Gabriel C., Arviset C., Ponz D., Solano E., eds, ASP Conf. Ser. Vol. 347, ADASS XIV, The D4A Digitiser. Astron. Soc. Pac., San Francisco, p. 651
De Cuyper J. P., Winter L., 2006, in Bohlenoler D., Durand D., Dowler P., eds, ASP Conf. Ser. Vol. 351, ADASS XV, The D4A digitiser. Astron. Soc. Pac., San Francisco, p. 587
De Cuyper J. P., Winter L., De Decker G., Zacharias N., Pascu D., Arlot J. E., Robert V., Lainey V., 2009, A&A, 335, 1111
Fienga A., 1998, A&A, 335, 1111
Fienga A., Manche H., Laskar J., Gastineau M., 2008, A&A, 477, 315
Fienga A. et al., 2009, A&A, 507, 1675
Fienga A., Manche H., Kuchynka P., Laskar J., Gastineau M., 2010, IMCCE Memorandum, INPOP10a
Folkner W. M., Williams J. G., Boggs D. H., 2008, JPL Memorandum IOM 343R-08-003, The planetary and Lunar ephemeris DE 421
Josties F. J., Dahn C. C., Kallarakal V. V., Miranian M., Douglass G. G., Christy J. W., Behall A. L., Harrington R. S., 1974, in Publ. United States Naval Observatory Vol. XXII, Part VI, Photographic measures of double stars.
Kaplan G. H., Hughes J. A., Seidelmann P. K., Smith C. A., Yallop B. D., 1989, AJ, 97, 1197
Lainey V., Arlot J. E., Karatekin O., Van Hoolst T., 2009, Nat, 459, 957
Lindegren L., 1977, A&A, 57, 55
Pascu D., 1977, in Burns J. A., ed., Planetary Satellites. Univ. Arizona Press, Tucson
Pascu D., 1979, in Nacozy P. E., Ferraz-Mello S., eds, Natural and Artificial Satellite Motion. Univ. Texas Press, Austin
Pascu D., 1994, in Morrison L. V., Gilmore G.F., eds, Galactic and Solar System Optical Astrometry. Cambridge Univ. Press, Cambridge
Pascu D., Schmidt R. E., 1990, AJ, 99, 1974
Urban S. E., Zacharias N., Wycoff G. L., 2004, Vizier On-Line Data Catalog, I/294A, The UCAC2 Bright Star Supplement (Urban+, 2006)
Winter L., 2005, Internal report (ROB and Hamburg)
Winter L., 2008, Internal report (ROB and Hamburg)
Zacharias N., Urban S. E., Zacharias M. I., Wycoff G. L., Hall D. M., Monet D. G., Rafferty T. J., 2004, AJ, 127, 3043
Zacharias N., Winter L., Holdenried E. R., De Cuyper J. P., Rafferty T. J., Wycoff G. L., 2008, in ASP Conf. Ser. Vol. 120, The StarScan Plate Measuring Machine: Overview and Calibrations. Astron. Soc. Pac., San Francisco, p. 644

This paper has been typeset from a TEX/LATEX file prepared by the author.